GJI Geomagnetism, rock magnetism and palaeomagnetism

Archaeointensity determinations from Italy: new data and the Earth's magnetic field strength variation over the past three millennia

Evdokia Tema,[1] Avto Goguitchaichvili[2] and Pierre Camps[3]

[1]*Dipartimento di Scienze della Terra, Università degli Studi di Torino, Torino, Italy. E-mail: evdokia.tema@unito.it*
[2]*Laboratorio Interinstitucional de Magnetismo Natural, Instituto de Geofísica, UNAM, Campus Morelia, Michoacan, Mexico*
[3]*Géosciences Montpellier, CNRS and Université Montpellier 2, Montpellier, France*

SUMMARY

Three kilns and a collection of baked bricks from Italian archaeological sites have been studied for archaeointensity determination using the Thellier method as modified by Coe. All sites are dated based on archaeological information and their ages range from 500 to 800 AD and 1500 to 1700 AD. Rock magnetic studies identify magnetite, Ti- magnetite and hematite as the main magnetic minerals, and magnetic susceptibility versus temperature shows a good thermal stability of the samples. The intensity results have been corrected for anisotropy of the thermoremanent magnetization and cooling rate effects. The new data together with 136 previously published results are used to estimate the variation of the Earth's magnetic field over the past three millennia. The time distribution of the Italian absolute intensity data is irregular with the majority of determinations concentrated during the last four centuries, while older periods are very poorly covered. Most of the data come from volcanic rocks and show significant discrepancies. All data have been compared with archaeointensity results from Europe and regional and global models predictions. This work indicates the need to obtain more high quality archaeointensity results, in particular for the periods older than 200 BC and between 200 and 1000 AD, in order to determine a robust Italian intensity secular variation curve that, in combination with directional data, could be used for archaeomagnetic dating.

Key words: Archaeomagnetism; Palaeointensity; Palaeomagnetic secular variation.

INTRODUCTION

The variation of the Earth's magnetic field strength in Italy is well known for the last two centuries, and particularly since 1880 when for the first time it was systematically measured at the observatory of Pola (Istria Peninsula, now Croatia). For earlier times, palaeomagnetism has to be used to retrieve its past evolution. Palaeomagnetic secular variation data may come from well-dated archaeological materials, volcanic rocks and undisturbed lake sediments. Italian lacustrine sediments have been used for the construction of secular variation curves for declination and inclination (Brandt *et al.* 1999) but they can only provide information as far as relative palaeointensity is concerned. Volcanic rocks from Vesuvius and Etna have been also widely used for retrieving past geomagnetic secular variations (Tanguy 1975; Rolph & Shaw 1986; Conte-Fasano *et al.* 2006) but their reliability is often disputable mainly due to problems related to their age determination and low success rate of palaeointensity experiments (Calvo *et al.* 2002; Conte-Fasano *et al.* 2006). Well-dated archaeological artefacts are, thus, by far the most suitable materials for archaeointensity studies, as they usually carry a stable thermoremanent magnetization (TRM) and show good thermochemical stability during heating. Although abundant archaeological remains

are available in Italy, reliable archaeointensity data are still scarce. In our knowledge, only seven studies (Aitken *et al.* 1988; Evans 1986, 1991; Hedley & Wagner 1991; Donadini & Pesonen 2007; Hill *et al.* 2007, 2008) have been published yielding a total of only 20 determinations.

Numerous archaeomagnetic data produced during the last decade have allowed the construction of secular variation (SV) curves for different areas in Europe (Gallet *et al.* 2002; Schnepp & Lanos 2005; Gómez-Paccard *et al.* 2006a; Márton & Ferencz 2006; Tema *et al.* 2006). Nevertheless, in most cases such curves only describe the directional variations of the Earth's magnetic field. Archaeointensity investigations are particularly scarce in comparison to directional data. A detailed description of the full geomagnetic vector is available for Bulgaria (Kovacheva *et al.* 1998, 2009). For Western Europe, Chauvin *et al.* (2000) have compiled an archaeointensity data set for the last two millennia but they concluded that many of the existing data might not be reliable. Genevey & Gallet (2002) have published an important number of intensity data from French pottery fragments dated between the 4th and 16th centuries; some of these data have been recently re-evaluated by Genevey *et al.* (2009) and together with new results, they have reconstructed the geomagnetic field intensity variations in France for the last 800 yr.

De Marco *et al.* (2008) have compiled a catalogue of archaeointensity data for the Eastern Mediterranean area and have proposed a geomagnetic field intensity variation curve for Greece for the last 7 millennia. Gómez-Paccard *et al.* (2008) have published an important number of new archaeointensity data from Spain. Together with the most reliable data previously published for Western Europe, they have obtained a compilation of 79 individual data points that have been treated by Bayesian statistical modelling to describe the evolution of geomagnetic field intensity in Western Europe for the past 2000 yr.

Available archaeomagnetic directional data, in some cases supplemented by volcanic and sedimentary palaeomagnetic data, have been used to compute global (Hongre *et al.* 1998; Korte & Constable 2003) and regional geomagnetic field models (Pavón-Carrasco *et al.* 2008a). Updated models now include palaeointensity information (Korte & Constable 2005; Pavón-Carrasco *et al.* 2008b; Pavón-Carrasco *et al.* 2009). Such models are rapidly improving but their consistency highly depends on the quantity, quality and geographic distribution of the reference data set. More high quality archaeointensity data are still necessary to increase the resolution of the models and enhance our knowledge of the geomagnetic field intensity variations in the past.

In this study, new archaeointensity results from three kilns and a collection of baked bricks coming from three Italian archaeological sites are presented. All sites are dated based on archaeological information and their ages range from 500 to 800 AD and 1500 to 1700 AD. These new results are of high quality, supported by cooling rate and anisotropy corrections. They cover previously very poorly studied time intervals and contribute to the enrichment of archaeointensity data in Italy. The new data have been incorporated into the Italian absolute intensity data from the literature and their significance in the context of regional and global model predictions is finally discussed.

ARCHAEOLOGICAL CONTEXT AND SAMPLES DESCRIPTION

The studied material comes from three well-preserved kilns; one excavated at Canosa (southern Italy) and two at the archaeological site of Foro Traiano at Rome, and from a collection of bricks from Saluzzo (northern Italy).

The Canosa kiln is a big rectangular kiln made by bricks, located in a religious complex related to the ancient church of St Sabino. According to archaeological evidence and historical sources, the whole ecclesiastic unit belongs to the Late Antique and Early Medieval periods. The studied kiln was used for the production of bricks for the construction of the nearby church, built during the episcopacy of St Sabino (514–566 AD) and it is thus archaeologically dated around 6th century AD. Oriented in situ hand samples from the kiln's walls were collected for directional analyses from which 11 specimens from eight samples were used for archaeointensity determination.

The archaeological site of Foro Traiano is situated in the historical centre of Rome and is the last and the most glorious of the Imperial Forums. At Foro Traiano, two brick kilns belonging to different time periods have been sampled. The first kiln, called here Roma 1, is situated at the southeast part of Foro Traiano, near the street 'Via dei Fori Imperiali'. According to the stratigraphy of the archaeological excavation, the kiln was probably used in two distinct periods. It was first constructed during early medieval times and at that time it was small and circular. On this initial structure a second phase of construction can be observed. The kiln was transformed in a bigger

rectangular kiln constructed by bricks and was reused around 15th century AD, as suggested by its stratigraphic position. A total of 11 independently oriented brick samples have been collected for directional studies and eight of them have been used for archaeointensity measurements. The second kiln, Roma 2, was brought to light after the archaeological excavation of 1997 and is situated near the Foro Traiano's market. It is a circular kiln used for the production of lime. According to archaeological evidence, mainly based on the ensuing ceramic fragments fill of the kiln, it is dated to 7th–8th century AD. The archaeointensity has been determined for four of the eight oriented brick samples collected. The directional results of Canosa, Roma 1 and Roma 2 kilns have been previously published by Tema *et al.* (2006) and are summarized here in Table 1.

Five bricks from an ancient wall situated at Saluzzo (northern Italy) have been also sampled for archaeointensity determination. The samples were not oriented. Their displacement from the place of their production and their occasional orientation in the construction of the wall made them lose their exact position during heating. No precise information is available about the kiln in which the bricks were produced, but at that period it was common to use materials produced in artisan laboratories not far from the construction. The brick wall is historically dated around 16th–17th century AD and it is suggested that the bricks used for its construction belong to the same time period.

In all cases, block samples have been collected and then drilled at the laboratory using an electric water-cooled rock drill. The samples were drilled perpendicular to their flat surface, interpreted as the top or the bottom of the brick (Fig. 1). A total of 40 cylindrical specimens of standard dimensions (diameter $= 25.4$ mm, height $= 22$ mm) have been prepared and studied for archaeointensity determination.

MAGNETIC MINERALOGY

Magnetic mineralogy experiments have been done at the ALP palaeomagnetic laboratory (Peveragno, Italy). Rock magnetic results for Canosa, Roma 1 and Roma 2 kilns have been presented by Tema *et al.* (2006) and Tema (2009) and are supplemented here by the magnetic mineralogy results from Saluzzo bricks.

Isothermal remanent magnetization (IRM) acquisition curves, back field curves, thermal demagnetization of three IRM components (Lowrie 1990) and low-field magnetic susceptibility versus temperature have been used for the identification of the samples' magnetic mineralogy and their thermal stability. The IRM was given with a pulse magnetizer by applying stepwise magnetic induction up to 1.6 T. Samples from Canosa, Roma 1 and Roma 2 kilns show similar magnetic properties. The IRM curves indicate that the saturation of magnetization is generally reached at low magnetic inductions varying from 0.2 to 0.4 T and almost no fraction remains unsaturated after 1.6 T (Fig. 2a). The backfield curves show coercivities of remanence ranging from 20 to 50 mT indicating the presence of a low-coercivity mineral (Fig. 2b). Thermal demagnetization of IRM components (Lowrie 1990) shows the dominating role of the magnetically soft fraction with unblocking temperatures ranging between 420 and 560 °C (Fig. 2c). These results point to magnetite or Ti-magnetite as the main magnetic carrier of the Canosa, Roma 1 and Roma 2 samples.

Saluzzo bricks are characterized by different magnetic properties. IRM acquisition curve shows that the magnetization increases rapidly at low fields, for example, 50–150 mT, but then it continues to increase up to high values of applied field and saturation

Table 1. Archaeointensity results.

| Site (age) | Sample | Specimen | $T_{\min}-T_{\max}$ (°C) | n | f | g | q | F (µT) | $\pm\sigma$ (µT) | F_{cr} (µT) cooling rate corrected | F_{atrm} (µT) anisotropy corrected | Site mean values | | | | | | | | | |
| | | | | | | | | | | | | Intensity results | | | | | Directional results Tema *et al.* (2006) | | | | |
												N	$F_{\mathrm{m}}\pm\sigma$ (µT)	$F_{\mathrm{cm}}\pm\sigma$ (µT)	VADM (10^{22} A m²)	VDM (10^{22} A m²)	N	D_{s}	I_{s}	α_{95}	k
Roma 1 (1480–1520 AD)	Brick T1	T1e	150–480	10	0.83	0.88	12.9	54.70	3.10	53.92	52.85	8	57.7 ± 2.6	53.6 ± 1.2	9.06	8.89	11	359.0	62.4	2.8	258
	Brick T2	T2d	200–560	12	0.83	0.88	16.9	54.71	2.37	54.2	53.66										
	Brick T4	T4d	150–480	10	0.84	0.88	13.3	58.38	3.20	57.78	56.04										
		T4e	150–480	10	0.83	0.88	14.2	58.45	3.00	57.58	54.7										
	Brick mean							58.42	0.05	57.68	55.37										
	Brick T5	T5d	150–560	13	0.91	0.9	32.5	60.38	1.50	60.18	52.36										
	Brick T7	T7d	150–560	13	0.83	0.91	21.5	55.08	1.90	54.71	51.97										
	Brick T8	T8d	150–510	11	0.85	0.87	29.5	60.40	1.51	58.98	53.67										
	Brick T10	T10d	200–450	8	0.71	0.81	33.8	56.70	0.95	56.2	53.96										
		T10e	150–480	10	0.86	0.84	45.1	58.24	0.90	60.38	56.15										
	Brick mean							57.47	1.09	58.29	55.05										
	Brick T11	T11d	150–560	13	0.86	0.9	60.15	60.15	0.80	60.15	53.53										
Saluzzo (1500–1700 AD)	Brick S1	S1–4a	20–540	13	0.83	0.86	31.5	59.21	1.35	57.82	51.46	5	50.5 ± 6	46.0 ± 3.4	7.55						
		S1–5a	20–560	14	0.85	0.87	39.1	59.43	1.23	58.3	50.14										
		S1–7a	150–540	12	0.59	0.87	12.9	58.21	2.32	55.04	50.09										
	Brick mean							58.95	0.65	57.05	50.56										
	Brick S2	S2–1a	20–560	14	0.89	0.86	29.1	50.18	1.33	48.99	44.58										
		S2–2a	20–540	13	0.87	0.83	24.6	50.52	1.49	49.97	46.47										
		S2–5a	20–560	14	0.86	0.86	22.7	54.47	1.78	52.95	47.65										
	Brick mean							51.72	0.23	50.63	46.23										
	Brick S3	S3–1b	20–560	14	0.93	0.91	38.6	50.55	1.11	50.21	48.2										
		S3–2b	20–560	14	0.9	0.9	32.2	50.64	1.28	50.49	46.45										
		S3–10b	200–560	12	0.68	0.89	15.9	55.94	2.11	55.04	48.98										
	Brick mean							52.38	0.54	51.91	47.88										
	Brick S4	S4–1a	150–510	11	0.54	0.83	18.6	44.43	1.06	43.97	42.65										
		S4–2a	150–390	7	0.39	0.73	14.3	45.66	0.91	44.86	43.52										
		S4–4a	150–390	7	0.39	0.73	6.3	45.15	2.04	44.58	43.69										
	Brick mean							45.08	0.62	44.47	43.28										
	Brick S5	S5–7a	150–560	13	0.85	0.88	20.6	43.89	1.59	43.59	41.85										
		S5–8	200–560	12	0.75	0.84	21.5	41.78	1.23	42.48	40.36										
		S5–9	150–560	13	0.95	0.84	32.1	47.24	1.17	47.18	44.35										
	Brick mean							44.30	2.75	44.42	42.18										
Roma 2 (600–800 AD)	Brick TR2	TR2	150–560	13	0.91	0.85	21.9	78.77	2.77	77.4	71.98	4	76.1 ± 3.1	73.4 ± 3.5	12.4	12.3	8	8.4	61.8	2.3	573
	Brick TR6	TR6	150–560	13	0.88	0.88	21.0	75.90	2.80	75.3	73.79										
	Brick TR7	TR7	150–390	7	0.68	0.82	14.6	78.01	2.97	78.81	78.02										
	Brick TR8	TR8	150–510	11	0.63	0.85	25.6	71.89	1.50	71.07	69.65										

Table 1. (*Continued.*)

Site (age)	Sample	Specimen	$T_{min}-T_{max}$ (°C)	n	f	g	q	F (μT)	±σ (μT)	F_{cr} (μT) cooling rate corrected	F_{atrm} (μT) anisotropy corrected	Site mean values									
												Intensity results					Directional results Tema *et al.* (2006)				
												N	$F_m \pm \sigma$ (μT)	$F_{cm} \pm \sigma$ (μT)	VADM (10^{22} A m²)	VDM (10^{22} A m²)	N	D_s	I_s	α_{95}	k
Canosa (500–600 AD)	Brick C1	C1a	150–480	10	0.8	0.85	10.9	61.83	3.84	62.31	56.7										
	Brick C1	C1b	150–480	10	0.79	0.86	12.0	60.75	3.43	60.92	57.26										
	Brick mean							61.29	0.76	61.61	56.98	8	67.1 ± 2.7	61.1 ± 3.2	10.41	11.6	9	359.4	51.3	3.1	279
	Brick C2	C2f	20–480	11	0.93	0.89	21.1	59.90	2.33	59.91	67.11										
	Brick C5	C5a	150–480	10	0.87	0.88	32.4	64.91	1.52	65.2	59.33										
	Brick C6	C6a	150–480	11	0.72	0.86	20.3	62.26	1.89	61.6	59.75										
	Brick C6	C6b	150–540	11	0.78	0.87	13.9	62.13	3.03	60.62	56.99										
	Brick mean							62.20	0.09	61.11	58.37										
	Brick C7	C7a	150–560	13	0.67	0.85	11.7	65.45	3.20	64.25	64.89										
	Brick C7	C7b	150–560	13	0.76	0.88	18.0	62.61	2.34	61.83	61.21										
	Brick mean							64.03	2.01	63.04	63.05										
	Brick C8	C8c	150–480	10	0.64	0.83	10.3	66.68	3.44	66.88	62.87										
	Brick C11	C11e	150–560	12	0.95	0.88	20.6	64.99	2.62	65.29	59.42										
	Brick C12	C12a	150–480	9	0.8	0.8	11.1	68.19	3.73	68.76	64.64										

Notes: Site (age), location of the archaeological site (archaeological age of the samples); Sample, name of samples; Specimen, name of specimens per sample; $T_{min} - T_{max}$, interval temperature used for the slope calculation; n, number of data points within the selected temperature interval; f, fraction of the NRM component used in the slope calculation; g, gap factor; q, quality factor; $F \pm \sigma$, palaeointensity estimate at specimen level and its standard deviation; F_{cr}, palaeointensity estimate after cooling rate correction; F_{atrm}, palaeointensity estimate after cooling rate and anisotropy correction; N, number of samples used for the calculation of the intensity mean; $F_m \pm \sigma$, mean palaeointensity estimate at site level and its standard deviation; F_{cm}, mean palaeointensity estimate after cooling rate and anisotropy correction; VADM, virtual axial dipole moment calculated using the mean intensities corrected for the cooling rate effect and anisotropy; VDM, virtual dipole moment calculated using the directional results from Tema *et al.* (2006); N, number of samples used for the calculation of the site mean direction; D_s, declination *in situ*; I_s, inclination *in situ*; α_{95}, 95% semi-angle of confidence; k, precision parameter. Geographic coordinates of the new sites: Roma (41.90° N, 12.45°E), Saluzzo (44.65° N, 7.48°E) and Canosa (41.22° N, 16.07°E).

is not reached at 1.6 T peak field (Fig. 2a). The backfield curve shows a high coercivity of remanence, around 220 mT, pointing to the presence of a high coercivity magnetic phase. Stepwise thermal demagnetization of a composite IRM according to Lowrie (1990) shows an important high coercivity component that significantly diminishes at around 200 °C and it is almost removed at around 600 °C. An important low coercivity component is also observed, removed at ~480 °C. The presence of two types of magnetic minerals is suggested: a low-coercivity mineral, probably magnetite or Ti-magnetite, and a high-coercivity mineral most likely hematite; both are very common in archaeological material like bricks, tiles and pottery.

The temperature dependence of low-field magnetic susceptibility from ambient temperature up to 700 °C is monitored using a Bartington MS2B susceptibility meter in combination with a MS2WF heating unit. Thermomagnetic curves are useful indicators for the thermal stability of baked materials. For all studied sites, the obtained heating and cooling curves, even if sometimes characterized by different shapes, are almost always reasonably reversible (Fig. 3). They indicate that no important mineralogical changes take place during heating and suggest that the bricks are magnetically stable.

ARCHAEOINTENSITY DETERMINATION

Experimental procedure

All archaeointensity measurements have been carried out at the LIMNA palaeomagnetic laboratory of UNAM (Campus Morelia, Mexico). The classical Thellier method (Thellier & Thellier 1959) modified by Coe (1967) and Coe *et al.* (1978) with regular partial thermoremanent magnetization (pTRM) checks was used. Samples were heated and cooled in a *ASC TD-48* oven and remanence was measured with a JR5 spinner magnetometer. A laboratory field of 50 μT was applied during heating and cooling along the cylindrical axis (z) of the samples. Generally, 10–12 temperature steps were performed from room temperature up to maximum 560 °C. Every two temperature steps a pTRM check was performed in order to detect any change in the pTRM acquisition capacity.

Archaeointensity data were interpreted using NRM-TRM plots (Fig. 4). Results are reported in Table 1 together with the statistical parameters calculated according to Coe *et al.* (1978) and the modifications proposed by Prévot *et al.* (1985). In Table 1, directional results from the Canosa, Roma 1 and Roma 2 kilns, as published by Tema *et al.* (2006), are also reported and used for the calculation of the virtual dipole moments (VDMs). The very high success rate of the archaeointensity determination (only two specimens rejected) demonstrates the excellent thermal stability of the samples, which is a common characteristic of archaeological materials (Chauvin *et al.* 2000; Gómez-Paccard *et al.* 2006b; De Marco *et al.* 2008). For the great majority of the specimens, linear NRM-TRM curves and positive pTRM checks are obtained (Fig. 4). No secondary component of magnetization was detected in the directional plots obtained from the palaeointensity experiment and the viscous magnetization, if any, was easily removed at 100–150 °C (Fig. 4). The high-quality NRM–TRM diagrams permit archaeointensity determinations based on more than half of the NRM component (f factor) and characterized by high values of quality parameters (Table 1). Only exceptions are specimens S4–2a and S4–4a (Saluzzo) that yield f factors lower than 0.5 (f = 0.39); however, they are still

Figure 1. Brick sample from Saluzzo. Samples were drilled perpendicular to their flat surface.
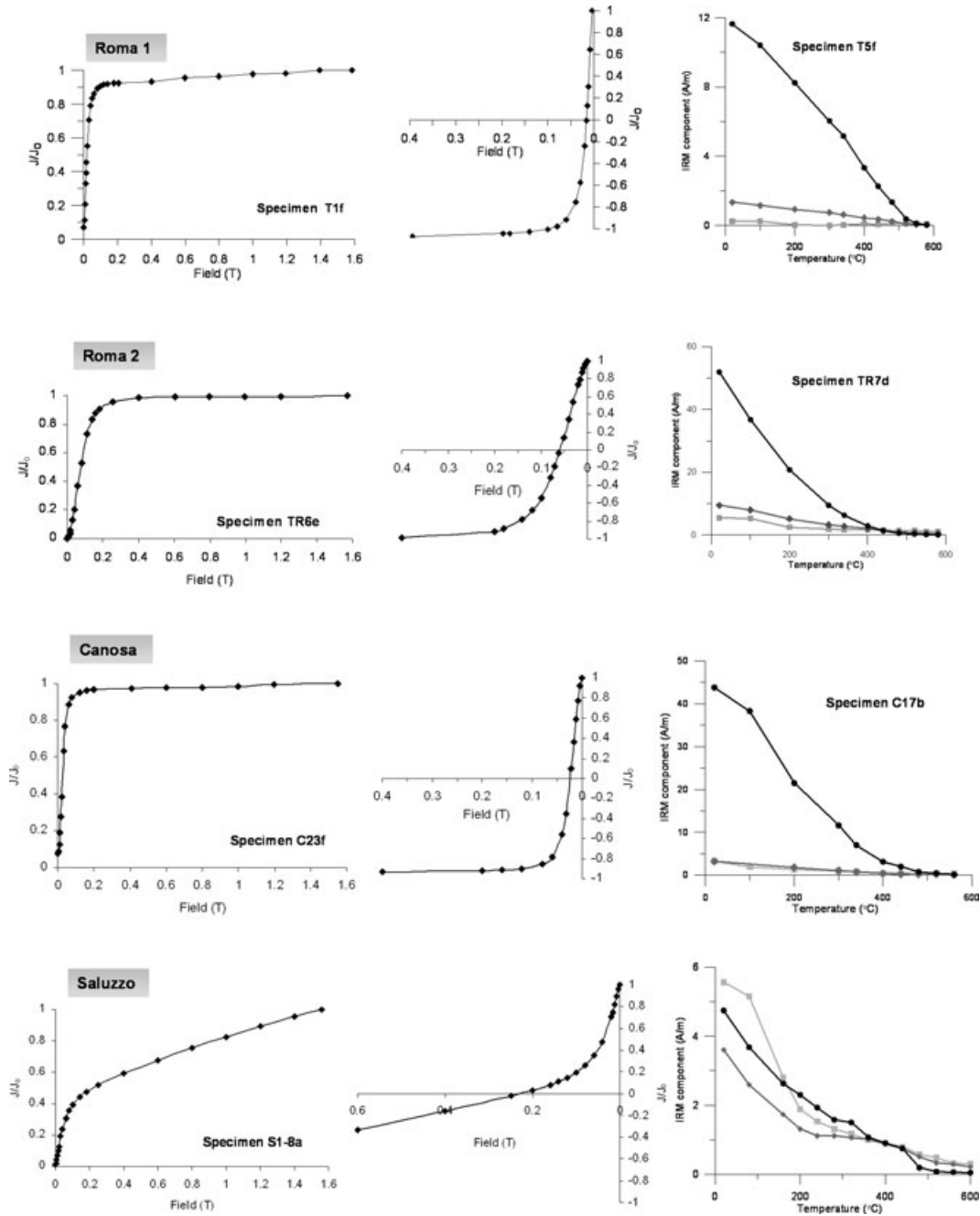

Figure 2. Examples of magnetic mineralogy experiments: (a) isothermal remanent magnetization (IRM) acquisition curves; (b) back field curves and (c) thermal demagnetization of three-axis IRM (Lowrie 1990). Symbols: black dot: low; grey diamond: intermediate; light grey square: high-coercivity component.
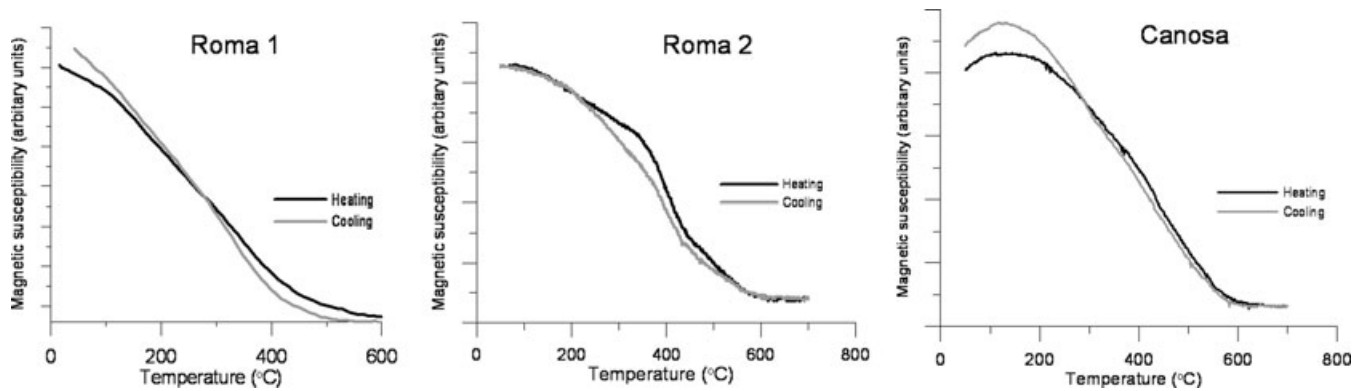
Figure 3. Representative magnetic susceptibility versus temperature curves. Heating (cooling) curve is illustrated in black (grey).

accepted as their archaeointensity values are very similar to other specimens from the same brick.

Cooling rate correction

During the archaeointensity experiments, the cooling time used is about one hour. Archaeological information, however, indicates that natural cooling time of the kilns after their use (or bricks after their production) is much higher and in some cases can be one day. It has been shown, both from theoretical considerations (Dodson & McClelland-Brown 1980; Halgedahl *et al.* 1980) and from experimental study (Fox & Aitken 1980) that the intensity of a TRM is significantly affected by the samples cooling rate.

In order to quantify the cooling rate effect in our samples, at the end of the archaeointensity experiments, all specimens were heated three more times at 560 °C in the presence of the same laboratory field used during the archaeointensity determination. First, the specimens were cooled using a quick cooling rate (1 hr), TRM_1; then, they were cooled using a longer cooling time ($\sim$12 hr) that is considered to approximate the natural slow cooling rate in our samples, TRM_2; and finally they were cooled once more with a quick cooling time (again 1 hr), TRM_3, as for TRM_1. The cooling rate effect is calculated as the difference between the fast and slow cooling time acquired magnetizations. It is expressed in percentage as

$$\Delta TRM \text{ (per cent)} = \frac{TRM_1 - TRM_2}{TRM_1} \text{(per cent)}.$$

The percentage variation between the intensity acquired during the two fast cooling rates, TRM_1 and TRM_3, is used to evaluate any change in TRM acquisition capacity caused by alteration during laboratory heating. The alteration factor is determined as

$$\text{Alteration factor (per cent)} = \frac{TRM_1 - TRM_3}{TRM_1} \text{(per cent)}.$$

In all our samples alteration factors are less than 2 per cent and the calculated cooling rate correction factors are very low, varying from 0 to 5 per cent (Table 1).

Anisotropy of thermoremanent magnetization (ATRM)

Baked clay artefacts, such as pottery, tiles and bricks, are often characterized by a strong magnetic anisotropy, mainly connected to their manufacture procedures (Rogers *et al.* 1979; Chauvin *et al.* 2000; Hus *et al.* 2002, 2004; Tema 2009). This anisotropy requires that the pTRM gained in Thellier's experiments is imparted with a

direction of the applied field as close as possible to the direction of the ancient field responsible for the NRM (Aitken *et al.* 1981). In practice, it is hardly possible to implement this constraint. This is mainly because, by definition in an anisotropic material, the remanence is more or less deviated towards the easy magnetization axis and thus, it does not mimic exactly the direction of the applied field. Therefore, the direction of the ancient field can not be accurately derived from the NRM, unless the anisotropy of remanence tensor is determined.

In this study, the magnetic anisotropy effect has been estimated by determining the TRM anisotropy tensor for all samples. ATRM measurements have been carried out at the palaeomagnetic laboratory of Géosciences Montpellier, by inducing a pTRM (560 °C to room temperature) in six sample directions (i.e. $+x$, $+y$, $+z$, $-x$, $-y$, $-z$). Subsequently to this sequence, a stability check was made by repeating a pTRM acquisition again in the $+x$ direction. Zero-field thermal demagnetizations at 570 °C before each pTRM were used as a baseline. The experimental conditions were as following: the samples were heated in a zero-field and cooled in a 50 μT (zero) field for magnetization (demagnetization), in two groups of 26 and 25 samples. The temperature repeatability between the seven in-field heatings was within 1.4 and 0.7 °C for the first and the second group, respectively. This control is ensured by means of three thermocouples placed at different positions within the heating chamber, plus three others sealed inside three dummy samples. Prior to the experiments, we calibrated the 50 μT induction field by measuring at room temperature its exact direction and magnitude every two cm along the sample holder within the heating chamber. The mean angle between the sample axes and the applied field is 0.3°, with a maximum value of 0.6°. These very low deviations guarantee very good experimental conditions. The residual field when a null field is required is less than 20 nT.

The ATRM results show a well-developed magnetic fabric that matches the bricks flat shape. The ATRM ellipsoid principal axes plotted in core coordinates (Fig. 5a) are characteristic of a flattening deformation, with maximum and intermediate ellipsoid axes lying parallel to the large face of the bricks and minimum axis systematically perpendicular to it. Most of the samples show oblate ellipsoid shape and the TRM anisotropy varies from 1.05 to 1.63 (Fig. 5b). Supported by a positive stability check (Fig. 6), an anisotropy correction factor has been calculated for each specimen according to Veitch *et al.* (1984). In our samples, the effect of TRM anisotropy is important and in some cases the corrected and uncorrected mean intensities differ by almost 9 per cent (Table 1).
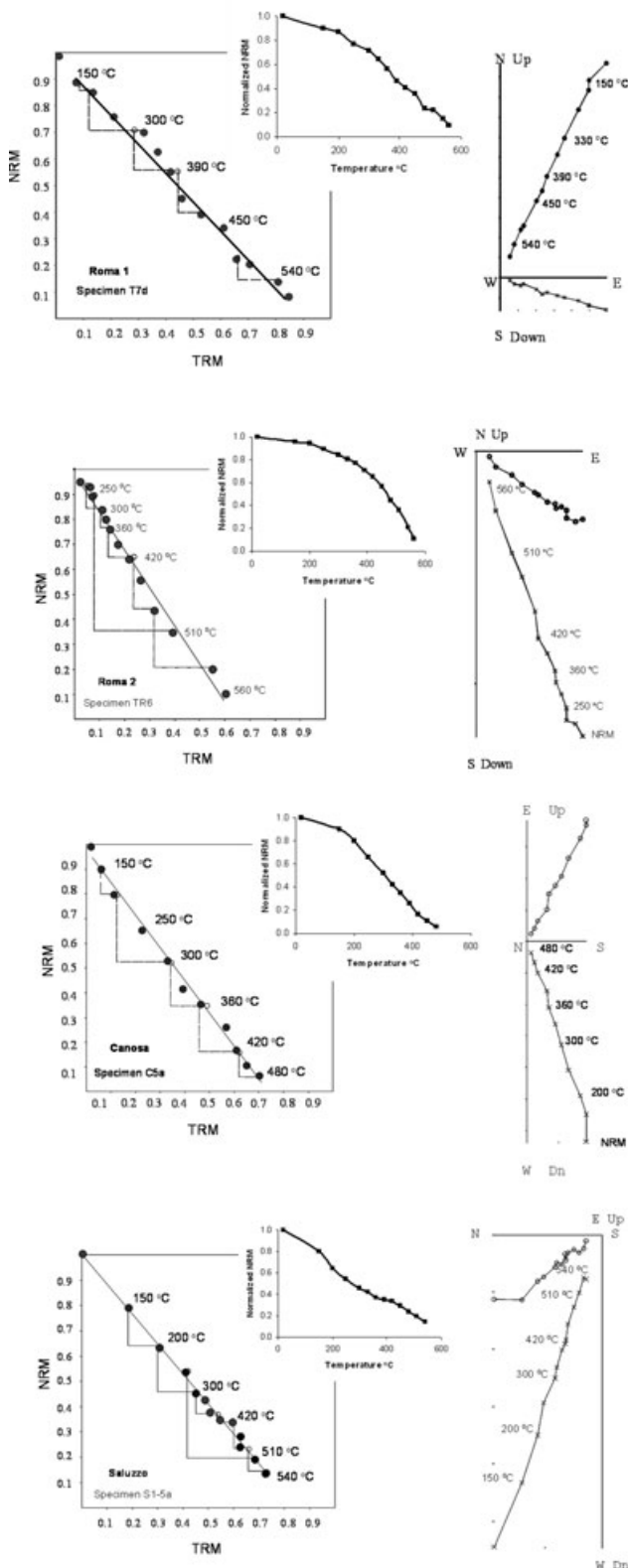
Figure 4. Representative examples of natural remanent magnetization/thermoremanent magnetization (NRM/TRM) diagrams together with the intensity decay curves and the corresponding orthogonal vector projections of the remanent magnetization in sample coordinates. Diagrams are normalized to the initial NRM intensity. In the orthogonal projections, the open (closed) dots refer to inclinations (declinations). During intensity experiments, pTRM-checks were performed every two thermal steps (small open circles in the NRM/TRM diagrams).
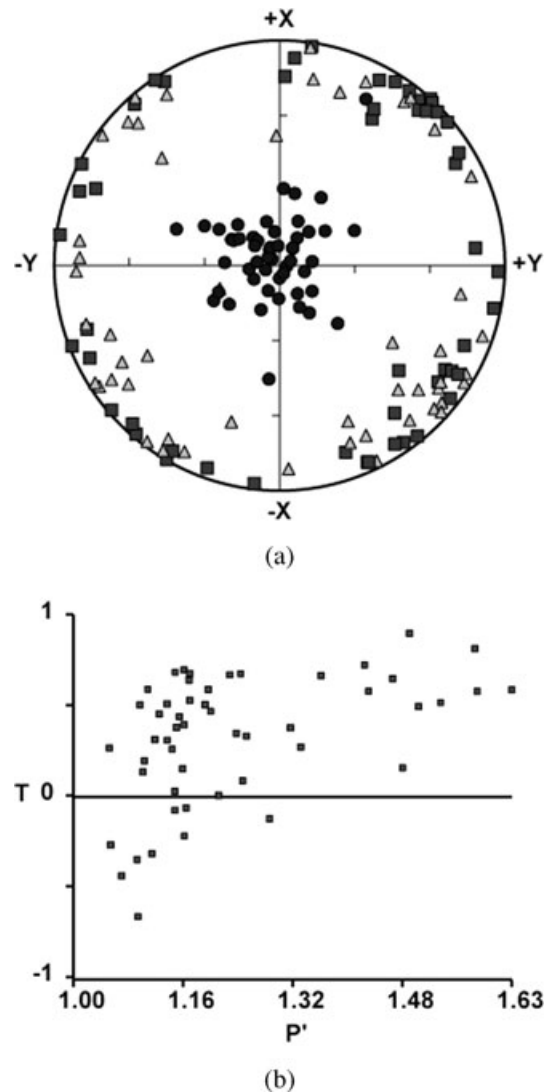
Figure 5. TRM anisotropy results for individual specimens. (a) Lower hemisphere equal-area plot of the ATRM ellipsoids principal axes in core coordinates. Symbols: dots: minimum; triangles: intermediate; squares: maximum principal axes. (b) ATRM ellipsoid shapes represented in a Jelinek (1981) projection.

NEW RESULTS AND ITALIAN ARCHAEOINTENSITY DATABASE FOR THE LAST 3000 YEARS

The difficulty in obtaining well-dated material for archaeomagnetic studies, the time-consuming experimental procedure for archaeointensity determination and its low success rate due to chemical changes during repeated heating, are some of the reasons for which published archaeointensity data are limited. Korhonen *et al.* (2008) have recently compiled a global intensity database (GEOMAGIA50) for the past 50 000 years including 3798 archaeomagnetic and palaeomagnetic intensity determinations. At the same time, Genevey *et al.* (2008) have updated the intensity database of Korte *et al.* (2005), presenting 3648 intensity data covering the past 10 millennia. The globally archaeointensity data available are much fewer than the 16 085 results of inclination and the 13 080 declination results published for the last 7 millennia (Korte *et al.* 2005).
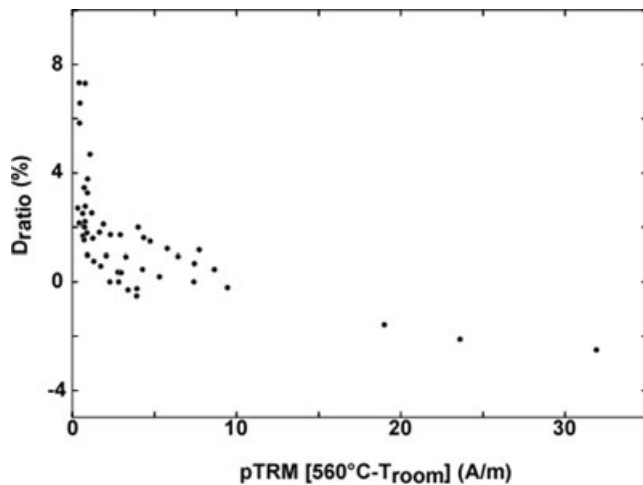
Figure 6. Stability check for TRM acquisition capacity. The D_{ratio}, expressed in percentage of the initial pTRM ($560\,°C - T_{room}$), corresponds to the difference between the pTRM acquired along the core *x*-axis, before and after the ATRM determination.
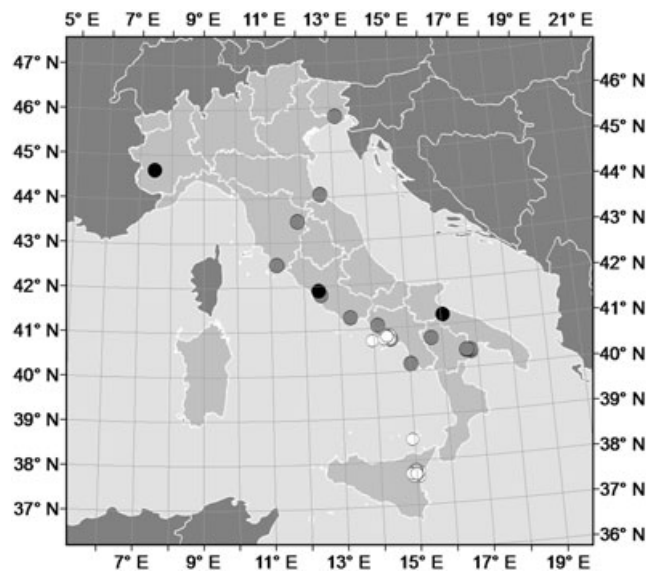

Figure 7. Geographical distribution of the Italian archaeointensity data. Symbols: black dot: new data; grey dot: data from literature coming from archaeological material; white dot: data from literature coming from volcanic rocks.

The Genevey *et al.* (2008) database includes 127 Italian intensity data coming from archaeological artefacts and lava flows. This data set has been here updated including archaeointensity results from some recent studies in Italy (Donadini & Pesonen 2007; Hill *et al.* 2007, 2008). Together with the new data presented in this study, a total of 140 Italian archaeointensity data are now available for the last 3000 yr. The geographical distribution of the data (Fig. 7) shows that they are concentrated in southern Italy and most of them come from lava flows from Vesuvius and Etna (83 per cent). Only the 17 per cent of the data come from archaeological material. Their time distribution is also irregular with the great majority of data concentrated at the last four centuries while older periods are very poorly covered (Fig. 8a). For the 1st millennium BC, only 12 data are available of which six come from the same archaeological site, where five contemporaneous kilns (200 BC–100 AD) from the same

workshop and a collection of amphorae samples have been studied (Hill *et al.* 2007). The 1st millennium AD is also poorly covered; only six data from the literature are available. The new data from Canosa and Roma 2, dated around 6th and 7–8th centuries AD, respectively, contribute to the enrichment of the data set, but our knowledge of the intensity variation in Italy for this period still remains very poor. Some centuries (e.g. 4–7th centuries BC and 3–4th and 9–11th AD) remain completely uncovered.

All data have been reduced at the latitude of Viterbo (42.45° N, 12.03°E) and plotted versus time (Fig. 8b). Lanza & Zanella (2003) proposed Viterbo repeat station (some 70 km from Rome) as the optimum reference point for relocating directional Italian secular variation data, as it is characterized by the smallest relocation error on both declination and inclination (±0.3°), whenever the original site is situated in Italy. For this reason, Tema *et al.* (2006) have relocated all Italian directional data to Vitebro and have used it as reference point for the construction of the master secular variation curve. To keep uniformity between the Italian directional and intensity data, we have also chosen Viterbo latitude to reduce the intensity results and we have checked the introduced intensity relocation error by using the Geomagnetic Field Maps of Italy (GMF) 2000 model (Coticchia *et al.* 2001). Saluzzo and Etna, the two most distant localities from Viterbo in the Italian intensity data set, were used to conduct this test. The difference between the reduced intensity and the direct intensity at Viterbo is in both cases less than 1.2 μT. This error is of the same order or even lower than the usual error associated to the palaeointensity determinations and can therefore be considered negligible.

Data coming from volcanic rocks are concentrated in the last 400 yr and show important discrepancies (Fig. 8b). Such difference may be due to dating problems often incurred in the case of volcanic rocks and/or to experimental errors during palaeointensity determination. A distortion of the geomagnetic field due to whole volcanic edifice is also possible. Some discrepancies are also observed at the intensity data from archaeological material for the period 300 BC–200 AD (Fig. 8b). For the period 200–1000 AD, only two data are available in the literature. Results from Canosa can be compared with the only datum available for the same age, coming from an obsidian lava flow from Lipari, dated at 543 ± 19 AD (Leonhardt *et al.* 2006). The Canosa archaeointensity is slightly higher than the one of the Lipari obsidian, but as already discussed by Leonhardt *et al.* (2006), the obsidian flow they investigated reveals an intensity value slightly lower than archaeomagnetic data from western Europe. Canosa's intensity is, however, in good coincidence with the intensity results from pottery coming from the archaeological site of Carlino, dated at 380–430 AD (Hedley & Wagner 1991). The new archaeointensity results from Roma 1 and Saluzzo are in very good coincidence with other data previously published for the same time period. No previously published data are available for comparison with Roma 2 results.

The new intensity results obtained in this study have been compared with the SCHA.DIF.3K archaeomagnetic model predictions for the last 3000 yr (Pavón-Carrasco *et al.* 2009). This is a recently proposed regional archaeomagnetic model that uses the available European database of archaeomagnetic field values and instrumental data to produce the geomagnetic field variations in Europe, modelling together the three geomagnetic elements: declination, inclination and intensity. The SCHA.DIF.3K model directly predicts the geomagnetic field at the site of interest, thus avoiding any eventual relocation error (Pavón-Carrasco *et al.* 2009). In the model's input database (essentially based on the database of Korte *et al.* 2005)
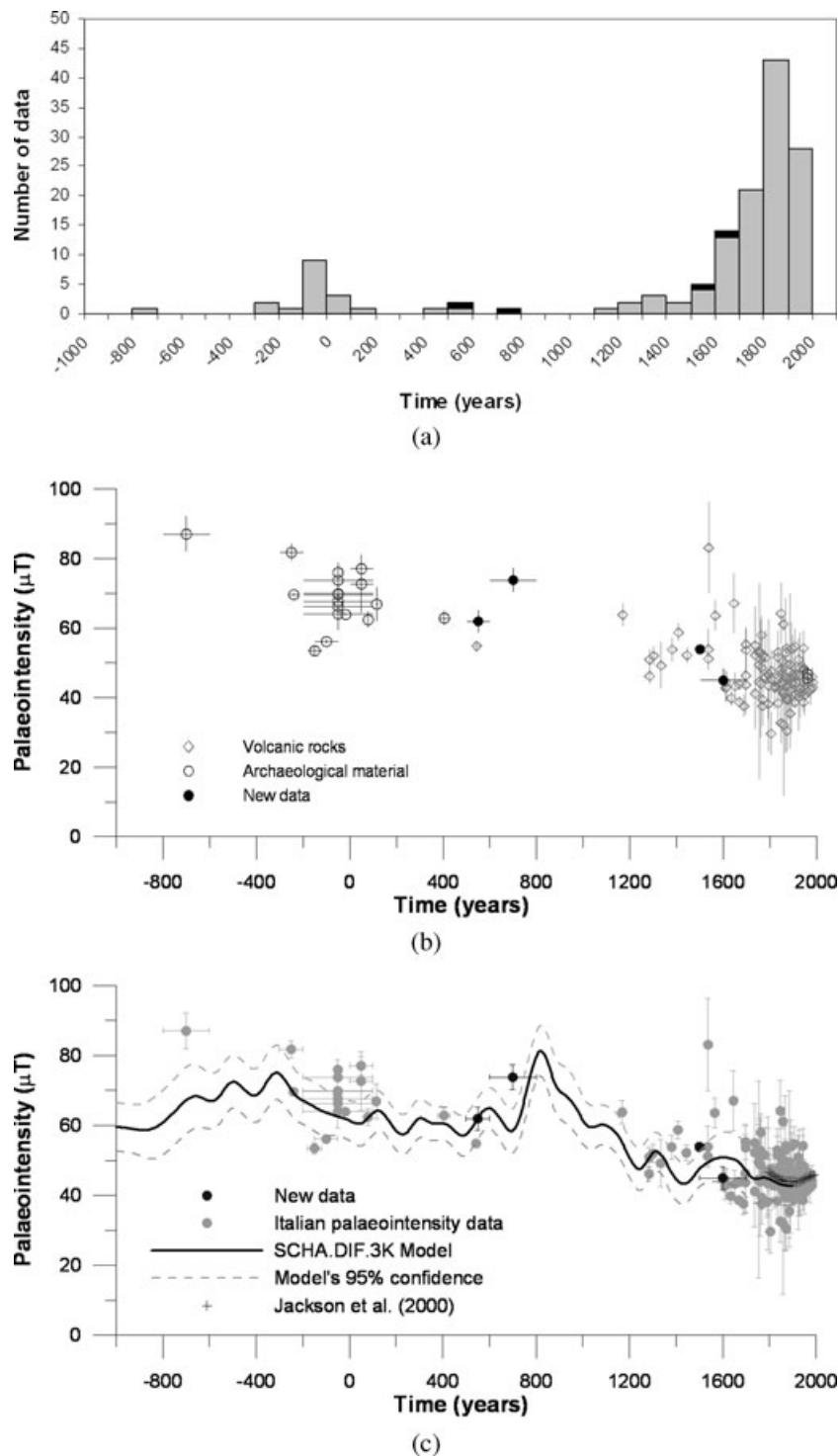
Figure 8. (a) Time distribution of the Italian archaeointensity data. Grey: data from literature; black: new data. (b) Italian archaeointensity data plotted versus age together with measurement error ($\pm\sigma$) and age uncertainties. Symbols: black dots: new data; open black dots: data from literature coming from archaeological material; open grey diamonds: data from literature coming from volcanic rocks. (c) Italian archaeointensity data plotted together with the SCHA.DIF.3K regional model intensity curve (Pavón-Carrasco *et al.* 2009). All data calculated at Viterbo (42.45°N, 12.03°E).

no data from Italian lava flows and only archaeomagnetic intensity data from Evans (1986, 1991) and Hedley & Wagner (1991) are included.

SCHA.DIF.3K model has been calculated directly at Viterbo and plotted with the Italian intensity data in Fig. 8(c). The in-

tensity curve for the last two centuries derived from the historical geomagnetic field model of Jackson *et al.* (2000) is also shown. Archaeointensity result from the Canosa kiln is in excellent agreement with the SCHA.DIF.3K model prediction for the 6th century AD. Agreement between the model and Roma's
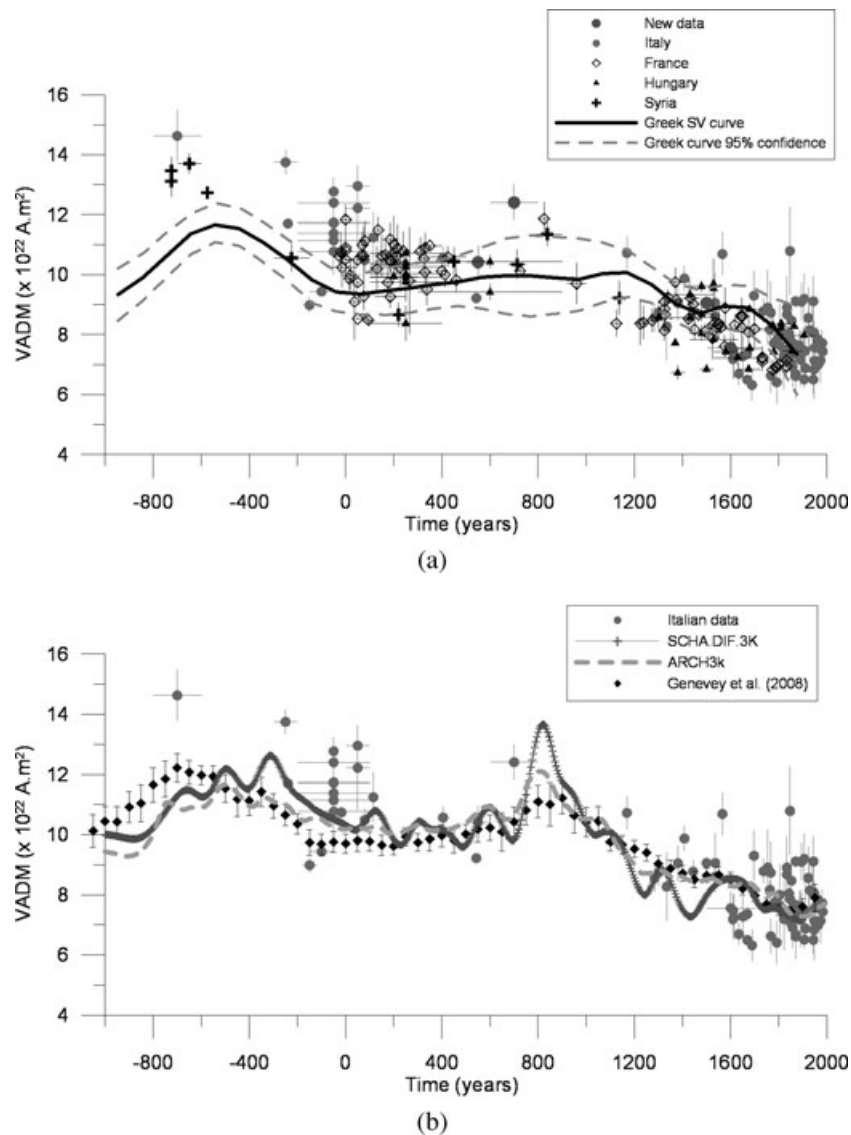
Figure 9. (a) Virtual axial dipole moments (VADMs) from Italy plotted together with VADMs values from France, Hungary, Syria (data from *ArcheoInt* database, Genevey *et al.* 2008) and the Greek intensity secular variation curve (De Marco *et al.* 2008), (b) comparison between VADMs from Italian data and VADMs predicted by the SCHA.DIF.3K regional model (Pavón-Carrasco *et al.* 2009), the ARCH3k (Korte *et al.* 2009) global model and the mean VADMs values from data from Western Europe (Genevey *et al.* 2008).

2 intensity can be noted but only if the kiln's age is shifted towards its upper limit (8th century AD). The Roma 1 and Saluzzo intensity results are within the model's 95 per cent confidence bar.

Comparison of the model's predictions with the Italian literature data shows a general agreement, but significant discrepancies can be observed. The intensity revealed by the 8–7th century BC Incoronata bricks, even if in good agreement with intensity data from Mesopotamia (Fig. 9a; Hill *et al.* 2008), is higher than the model's intensity. Higher intensity values are also recorded by two kilns from southern Italy dated to the 1st century AD (Evans 1986; note that these data are included in the model's input dataset). The kilns studied at Albinia by Hill *et al.* (2007), dated at 2nd century BC–1st century AD, fit the model curve if shifted nearer to the older half of their archaeological age, as already suggested by the authors and supported by the inclination data (Hill *et al.* 2007). However, some short-term variations predicted by the model (i.e. short intensity de-

crease at 1st and 13th century AD) are not supported by the Italian data.

For more recent periods, mainly covered by volcanic data, good agreement with the curve can be observed for the 14th century AD, but for the 16th–19th centuries data are scattered (Fig. 8c). Lava archaeointensities from the last two centuries compared with geomagnetic field intensity variation from historical measurements (Jackson *et al.* 2000), clearly show that not all data can be considered reliable. Genevey *et al.* (2008) have proposed various selection criteria for eliminating intensity data that do not fulfil reliability standards. In the case of Italian archaeointensity data, we have applied two data quality criteria based on the standard deviation values and the number of samples, eliminating all data with standard deviations higher than 15 per cent and those where the intensity determination comes from only one sample. Following these criteria, 44 data have been rejected, all of them coming from recent lava flows.

COMPARISON WITH ARCHAEOINTENSITY RESULTS FROM EUROPE AND GLOBAL MODEL PREDICTIONS

The virtual axial dipole moments (VADMs) have been calculated for the Italian archaeointensity data that fulfil the basic selection criteria discussed above and they have been compared with the VADM values from France, Hungary and Syria (Fig. 9a; data from *ArcheoInt* database, updated with Genevey *et al.* (2009) recently published French data). In Fig. 9(a) the Greek secular variation curve (De Marco *et al.* 2008) accompanied with an error envelope at a 95 per cent confidence level, obtained according to the hierarchical Bayesian modelling (Lanos *et al.* 2005), has been also added for comparison. Such comparison confirms a good agreement between the new data from Roma 1 and Saluzzo and those obtained from France and Hungary for 15th and 16th centuries, respectively. The VADM calculated from the Canosa kiln intensity is in good agreement with the VADM value from a study in Hungary and the Greek SV curve. For the 8–9th century AD, despite the addition of the Roma 2 result, data still remain scatter. There are two low VADMs estimated by Syrian (Genevey *et al.* 2003) and French potsherd (Genevey & Gallet 2002) and three higher values coming from Syria, France and Italy (Roma 2 kiln). The Greek SV curve does not offer much more information because for this period only few Greek data are available (Papamarinopoulos 1987; Aitken *et al.* 1989) and the Greek SV curve is characterized by large error envelope (De Marco *et al.* 2008).

During last decade, a significant number of continuous global spherical harmonic models of the geomagnetic field have been proposed (Korte & Constable 2003, 2005; Korte *et al.* 2009). CALS3k is the most recently proposed model (Korte *et al.* 2009), based on the updated global database published by Donadini *et al.* (2009) that includes data from archaeological material, lava flows and lake sediments. Korte *et al.* (2009) have also proposed the ARCH3k archaeomagnetic model that follows the same modelling concept with CALS3k, but uses only data from archaeological material and volcanic rocks. ARCH3k has, thus, slightly higher resolution and is considered more reliable for archaeomagnetic applications than the models including sediment records (Korte *et al.* 2009). For this reason, the ARCH3k model has been used here for comparison with the virtual axial dipole moments from Italian archaeomagnetic data (Fig. 9b). In Fig. 9(b), the VADM mean values from Western Eurasian data, computed using sliding windows of 100 yr shifted by 50 yr (Genevey *et al.* 2008) and the VADMs from the regional SCHA.DIF.3K geomagnetic field model (Pavón-Carrasco *et al.* 2009) computed at Viterbo are also plotted. For the last four centuries all models are in good agreement with each other showing low VADM values; Italian lava data for the same period, even though quite dispersed, do confirm this VADM decrease. For older times, some discrepancies can be observed. SCHA.DIF.3K and ARCH3k clearly show high VADMs for the 9th century AD. However, the only datum available from Italy for the 9th century is not enough to support the intensity peak. More data for this period are necessary to justify this intensity increase predicted by the models that for the moment does not seem realistic. The model predictions from 0 to 600 AD show very small VADM variations, and lower values than those calculated from Italian data available for the 100 BC–100 AD period. For older BC times, the Italian archaeointensity data are extremely scarce.

CONCLUSIONS

Four new high quality archaeointensity data corrected for anisotropy and cooling rate effects have been obtained from Italian archaeological material. These new data together with an updated compilation of previously published Italian archaeointensity data have been used for the reconstruction of the geomagnetic field intensity in Italy over the last 3000 yr. Data from volcanic rocks, mainly coming from historical eruptions in the last four centuries, show important discrepancies, pointing out that lava flows should be used in secular variation studies with caution. On the other hand, data coming from archaeological material are very sparse. Undoubtedly, more data are clearly needed in order to establish a reliable intensity reference curve for Italy. In particular, high quality archaeointensity determinations of well-dated archaeological artefacts are necessary for the time period 200–1000 AD and periods older than 200 BC. Improvement of the geographic distribution is also necessary. Enrichment of data is critical for the construction of reliable global and regional models in order to be used for archaeomagnetic dating.

REFERENCES

Aitken, M.J., Alcock, P., Bussel, G. & Shaw, C., 1981. Archaeomagnetic determination of the past geomagnetic intensity using ancient ceramics: allowance for anisotropy, *Archaeometry,* **23,** 53–64.

Aitken, M.J., Allsop, A.L., Bussell, G.D. & Winter, M.B., 1988. Determination of the intensity of the Earth's magnetic field during archaeological times: reliability of the Thellier technique, *Rev. Geophys.,* **26,** 3–12.

Aitken, M.J., Allsop, A.L., Bussell, G.D., Liritzis, Y. & Winter, M.B., 1989. Geomagnetic intensity measurements using bricks from Greek churches of the first and second millennia AD, *Archaeometry,* **31,** 77–87.

Brandt, U., Nowaczyk, N.R., Ramrath, A., Brauer, A., Mingram, J., Wulf, S. & Negendank, J.F.W., 1999. Palaeomagnetism of Holocene and Late Pleistocene sediments from Lago di Mezzano and Lago Grande di Monticchio (Italy): initial results, *Quater. Sci. Rev.,* **18,** 961–976.

Calvo, M., Prévot, M., Perrin, M. & Riisager, J., 2002. Investigating the reasons for the failure of palaeointensity experiments: a study on historical lava flows from Mt. Etna (Italy), *Geophys. J. Int.,* **149,** 44–63.

Chauvin, A., Garcia, Y., Lanos, P.H. & Laubenheimer, F., 2000. Paleointensity of the geomagnetic field recovered on archaeomagnetic sites from France, *Phys. Earth planet. Inter.,* **120,** 111–136.

Coe, R.S., 1967. Paleo-intensities of the Earth's magnetic field determined from Tertiary and Quaternary rocks, *J. geophys. Res.,* **72**(12), 3247–3262.

Coe, R.S., Grommé, S. & Mankinen, E.A., 1978. Geomagnetic paleointensities from radiocarbon-dated lava flows on Hawaii and the question of the Pacific nondipole low, *J. geophys. Res.,* **83**(B4), 1740–1756.

Conte-Fasano, G., Urrutia-Fucugauchi, J., Goguitchaichvili, A., Incoronato, A. & Tiano, P., 2006. Lava identification by palaeomagnetism: a case study and some problems surrounding the 1631 eruption of Mount Vesuvius, Italy, *Earth Planets Space,* **58,** 1061–1069.

Coticchia, A., De Santis, A., Di Ponzio, A., Dominici, G., Meloni, A., Pierozzi, M. & Sperti, M, 2001. Italian magnetic network and geomagnetic field maps of Italy at year 2000, *Bollettino di geodesia e scienze affini,* **4,** Anno LX, 261–291.

De Marco, E., Spatharas, V., Gómez-Paccard, M., Chauvin, A. & Kondopoulou, D., 2008. New archaeointensity results from archaeological sites and variation of the geomagnetic field intensity for the last 7 millennia in Greece, *Phys. Chem. Earth,* **33,** 578–595.

Dodson, M.H. & McClelland-Brown, E., 1980. Magnetic blocking temperatures of single domain grains during slow cooling, *J. geophys. Res.,* **96,** 1981–2006.

Donadini, F. & Pesonen, L., 2007. Archeointensity determinations from Finland, Estonia and Italy, *Geophysica,* **43**(1–2), 3–18.

Donadini, F., Korte, M. & Constable, C.G., 2009. Geomagnetic field for 0–3 ka: 1. New data sets for global modelling, *Geochem. Geophys. Geosyst.,* **10,** Q06007, doi:10.1029/2008GC002295.

Evans, M.E., 1986. Paleointensity estimates from Italian kilns, *J. Geomag. Geoelectr.,* **38,** 1259–1267.

Evans, M.E., 1991. An archaeointensity investigation of a kiln at Pompeii, *J. Geomag. Geoelectr.,* **43,** 357–361.

Fox, J.M.W. & Aitken, M.J., 1980. Cooling-rate dependence of thermoremanent magnetisation, *Nature,* **283,** 262–361.

Gallet, Y., Genevey, A. & Le Goff, M., 2002. Three millennia of directional variation of the Earth's magnetic field in Western Europe as revealed by archaeological artefacts, *Phys. Earth planet. Inter.,* **131,** 81–89.

Genevey, A. & Gallet, Y., 2002. Intensity of the geomagnetic field in western Europe over the past 200 years: new data from ancient French pottery, *J. geophys. Res.,* **107**(B11), 2285, doi:10.1029/2001JB000701.

Genevey, A., Gallet, Y. & Margueron, J.C., 2003. Eight thousand years of geomagnetic field intensity variations in the eastern Mediterranean, *J. geophys. Res.,* **108**(B5), 2228, doi:10.1029/2001JB001612.

Genevey, A., Gallet, Y., Constable, C., Korte, M. & Hulot, G., 2008. ArcheoInt: an upgraded compilation of geomagnetic field intensity data for the past ten millennia and its application to the recovery of the past dipole moment, *Geochem. Geophys. Geosyst.,* **9**(4), Q04038, doi:10.1029/2007GC001881.

Genevey, A., Gallet, Y., Rosen, J. & Le Goff, M., 2009. Evidence for rapid geomagnetic field intensity variations in Western Europe over the past 800 years from new French archaeointensity data, *Earth planet. Sci. Lett.,* **284,** 132–143.

Gómez-Paccard, M., Chauvin, A., Lanos, P., McIntosh, G., Osete, M.L., Catanzariti, G., Ruiz-Martínez, V.C. & Núñez, J.I., 2006a. The first archaeomagnetic secular variation curve for the Iberian Peninsula. Comparison with other data from Western Europe and with global geomagnetic field models, *Geochem. Geophys. Geosyst.,* **7,** Q12001, doi:10.1029/2006GC001476.

Gómez-Paccard, M., Chauvin, A., Lanos, P., Thiriot, J. & Jiménez-Castillo, P., 2006b. Archaeomagnetic study of seven contemporaneous kilns from Murcia (Spain), *Phys. Earth planet. Inter.,* **157,** 16–32.

Gómez-Paccard, M., Chauvin, A., Lanos, P.H. & Thiriot, J., 2008. New archaeointensity data from Spain and the geomagnetic dipole moment in western Europe over the past 2000 years, *J. geophys. Res.,* **113,** B09103, doi:10.1029/2008JB005582.

Halgedahl, S.L., Day, R. & Fuller, M., 1980. The effect of cooling rate intensity of week-field TRM in single-domain magnetite, *J. geophys. Res.,* **85,** 3690–3698.

Hedley, I. & Wagner, G.C., 1991. A magnetic investigation of Roman and pre-Roman pottery, in *Archaeometry'90,* pp. 275–284, eds Pernicka, E. & Wagner, G.C., Basel.

Hill, M., Lanos, P.H., Chauvin, A., Vitali, D. & Laubenheimer, F., 2007. An archaeomagnetic investigation of a Roman amphorae workshop in Albinia (Italy), *Geophys. J. Int.,* **169,** 471–482.

Hill, M., Lanos, P.H., Denti, M. & Dufresne, P.H., 2008. Archaeomagnetic investigation of bricks from the VIIIth–VIIth century BC Greek-indigenous site of Incoronata (Metaponto, Italy), *Phys. Chem. Earth,* **33,** 523–533.

Hongre, L., Hulot, G. & Khokhlov, A., 1998. An analysis of the geomagnetic field over the past 2000 years, *Phys. Earth planet. Inter.,* **106,** 311–335.

Hus, J., Ech-Chakrouni, S. & Jordanova, D., 2002. Origin of magnetic fabric in bricks: its implications in archaeomagnetism, *Phys. Chem. Earth,* **27,** 1319–1331.

Hus, J., Geeraerts, R. & Plumier, J., 2004. On the suitability of refractory bricks from a Mediaeval brass melting and working site near Dinant (Belgium) as geomagnetic field recorders, *Phys. Earth planet. Inter.,* **147,** 103–116.

Jackson, A., Jonkers, A. & Walker, M., 2000. Four centuries of geomagnetic secular variation from historical records, *Phil. Trans. R. Soc. Lond., Ser. A,* **358,** 957–990.

Jelinek, V., 1981. Characterization of the magnetic fabric of rocks, *Tectonophysics,* **79,** 63–67.

Korhonen, K., Donadini, F., Riisager, P. & Pesonen, L.J., 2008. GEOMAGIA50: an archeointensity database with PHP and MySQL, *Geochem. Geophys. Geosyst.,* **9,** Q04029, doi:10.1029/2007GC001893.

Korte, M. & Constable, C.G., 2003. Continuous global geomagnetic field models for the past 3000 years, *Phys. Earth planet. Inter.,* **140,** 73–89.

Korte, M. & Constable, C.G., 2005. Continuous geomagnetic field models for the past 7 millennia: 2.CALS7K, *Geochem. Geophys. Geosyst.,* **6,** Q02H16, doi:10.1029/2004GC000801.

Korte, M., Genevey, A., Constable, C., Frank, U. & Schnepp, E., 2005. Continuous geomagnetic field models for the past 7 millennia: 1. A new global data compilation, *Geochem. Geophys. Geosyst.,* **6,** Q02H15, doi:10.1029/2004GC000800.

Korte, M., Donadini, F. & Constable, C.G., 2009. Geomagnetic field for 0–3 ka: 2. A new series of time-varying global models, *Geochem. Geophys. Geosyst.,* **10,** Q06008, doi:10.1029/2008GC002297.

Kovacheva, M., Jordanova, N. & Karloukovski, V, 1998. Geomagnetic field variations as determined from Bulgarian archaeomagnetic data. Part II: the last 8000 years, *Surv. Geophys.,* **19,** 431–460.

Kovacheva, M., Boyadziev, Y., Kostadinova-Avramova, M., Jordanova, N. & Donadini, F., 2009. Updated archaeomagnetic data set of the past 8 millennia from the Sofia laboratory, Bulgaria, *Geochem. Geophys. Geosyst.,* **10,** Q05002, doi:10.1029/2008GC002347.

Lanos, Ph., Le Goff, M., Kovacheva, M. & Schnepp, E., 2005. Hierarchical modelling of archaeomagnetic data and curve estimation by moving average technique, *Geophys. J. Int.,* **160,** 440–476.

Lanza, R. & Zanella, E., 2003. Palaeomagnetic secular variation at Vulcano (Aeolian Islands) during the last 135 kyr, *Earth planet. Sci. Lett.,* **213,** 312–336.

Leonhardt, R., Matzka, J., Nichols, A.R.L. & Dingwell, D.B., 2006. Cooling rate correction for paleointensity determination for volcanic glasses by relaxation geospeedometry, *Earth planet. Sci. Lett.,* **243,** 282–292.

Lowrie, W., 1990. Identification of ferromagnetic minerals in a rock by coercivity and unblocking temperature properties, *Geophys. Res. Lett.,* **17,** 159–162.

Márton, P. & Ferencz, E., 2006. Hierarchical versus stratification statistical analysis of archaeomagnetic directions: the secular variation curve for Hungary, *Geophys. J. Int.,* **164,** 484–489.

Papamarinopoulos, S., 1987. Geomagnetic intensity measurements from Byzantine vases in the period between 300 and 1650 yr. A.D, *J. Geomag. Geoelectr,* **39,** 261–270.

Pavón-Carrasco, F.J., Osete, M.L., Torta, J.M., Gaya-Piqué, L.R. & Lanos, P.H., 2008a. Initial SCHA.DI.00 regional archaeomagnetic model for Europe for the last 2000 years, *Phys. Chem. Earth,* **33**(6–7), 596–608.

Pavón-Carrasco, F.J., Osete, M.L., Torta, J.M. & Gaya-Piqué, L.R., 2008b. A regional archaeomagnetic model for the palaeointensity in Europe for the last 2000 years and its implications for climatic change, *Pure appl. Geophys.,* **165**(6), 1209–1225, doi:10.1007/s00024–008-0354–4.

Pavón-Carrasco, F.J., Osete, M.L., Torta, J.M. & Gaya-Piqué, L.R., 2009. A regional archaeomagnetic model for Europe for the last 3000 years, SCHA.DIF.3K: applications to archaeomagnetic dating, *Geochem. Geophys. Geosyst.,* **10**(3), Q03013, doi:10.1029/2008GC002244.

Prévot, M., Mankinen, E.A., Coe, R.S. & Grommé, C.S., 1985. The Steens mountain (Oregon) geomagnetic polarity transition. 2. Field intensity variations and discussion of reversal models, *J. geophys. Res.,* **90,** 10 417–10 448.

Rogers, J., Fox, J.M.W. & Aitken, M.J., 1979. Magnetic anisotropy in ancient pottery, *Nature,* **277,** 644–646.

Rolph, T.C. & Shaw, J., 1986. Variations of the geomagnetic field in Sicily, *J. Geomag. Geoelectr.,* **38,** 1269–1277.

Schnepp, E. & Lanos, P.H., 2005. Archaeomagnetic secular variation in Germany during the past 2500 years, *Geophys. J. Int.,* **163,** 479–490.

Tanguy, J.C., 1975. Intensity of the geomagnetic field from recent Italian lavas using a new paleointensity method, *Earth planet. Sci. Lett.,* **27,** 314–320.

Tema, E., 2009. Estimate of the magnetic anisotropy effect on the archaeomagnetic inclination of ancient bricks, *Phys. Earth planet. Inter.,* **176,** 213–223.

Tema, E., Hedley, I. & Lanos, P., 2006. Archaeomagnetism in Italy: a compilation of data including new results and a preliminary Italian secular variation curve, *Geophys. J. Int.,* **167,** 1160–1171.

Thellier, E. & Thellier, O., 1959. Sur l'intensité du champ magnétique terrestre dans le passé historique et géologique, *Ann. Geophys.,* **15,** 285–376.

Veitch, R.J., Hedley, I.G. & Wagner, J.J., 1984. An investigation of the intensity of the geomagnetic field during Roman times using magnetically anisotropic bricks and tiles, *Arch. Sci. (Geneva),* **37**(3), 359–373.